JMEPEG (2008) 17:395–401
DOI: 10.1007/s11665-008-9224-6

1059-9495/$19.00

Shear Localization and Damage in AA5754 Aluminum Alloy Sheets

Jidong Kang, David S. Wilkinson, Mike Bruhis, Mukesh Jain, Pei Dong Wu, J. David Embury, Raja K. Mishra, and Anil K. Sachdev

(Submitted January 28, 2008; in revised form February 26, 2008)

In this article, we study the Portevin-Le Chatelier (PLC) bands and their influences on strain localization and fracture in continuous cast (CC) AA5754 aluminum sheets. Three types of tensile tests are conducted: (1) tensile samples are pulled directly to fracture at 223 K, (2) tensile samples are pulled at 223 K to initiate diffuse necking followed by unloading and reloading to fracture at room temperature, and (3) tensile samples are pulled at 223 K to localized necking and unloaded followed by reloading to fracture at room temperature. Furthermore, in situ V-bending test coupled with deformation mapping using digital image correlation is used to study damage at large strains. The results show that PLC bands detect favorable geometrical sites for shear band initiation. The formation of shear bands precedes damage and damage is a consequence of shear band formation.

Keywords aluminum, automotive, dynamic strain aging, mechanical testing, shear localization

1. Introduction

Aluminum alloys are finding increasing usage in the transportation industry because of their combination of low density, high strength, and good formability. Continuous cast (CC) AA5754 sheets are being produced to reduce cost of the final products in automotive applications. The onset of failure in aluminum sheets, especially CC sheets, remains a challenge for increased applications involving complex shapes as in body panel applications.

There are two types of shear localizations in solid solution alloys such as the Al-Mg system, namely Portevin-Le Chatelier (PLC) effect and shear bands. An evidence of PLC effect is the serrated flow in the tensile curves which occurs over a wide range of temperatures and strain rates. It is also well known that Al-Mg alloys fail by localization of flow into bands of intense shear (Ref 1-6). However, the mechanism governing the formation of shear bands is still controversial in the literature and current models cannot account for many experimental observations (Ref 7). For example, very little damage is seen just underneath the fracture surface that is dominated by void sheeting (Ref 8). The relationship between shear localization and damage in aluminum, for example, is different from that in steel. Furthermore, the relationship between PLC bands and shear bands needs further elucidation (Ref 9).

As the progress from necking to fracture occurs over a very small strain range during tensile deformation of aluminum alloys compared to steels, new experimental test methods are needed to examine the processes at work leading to failure. Failure in bending is controlled by fracture, while necking is the precursor to failure in tensile tests. Therefore, the bend testing provides an alternative way to observe damage in the absence of shear bands at large strains. A new instrumentally controlled bending fixture in which load-displacement curves can be recorded during the bending process (Ref 10) can be used to follow processes at large strains. Similarly, PLC bands can be suppressed at lower temperatures and/or higher strain rates, and the relationship between PLC bands and shear bands can be investigated by combining low temperature testing with room temperature tests.

In the present study, tensile tests were first carried out at 223 K to isolate PLC bands from shear bands, providing an opportunity to follow the deformation pattern that leads to the shear banding process. Tensile samples were then pulled to diffuse and localized necking at 223 K, and the deformation was continued at room temperature to delineate the relationship between PLC bands and shear bands. In situ V-bending test coupled with deformation mapping using digital image correlation (DIC) was used to reveal damage mechanisms at large strains.

1.1 Experiment

The material used for the present study was a commercially produced 2-mm-thick continuous cast AA5754-O sheet from Novelis. The chemical composition of the material was Al-3.1Mg-0.25Mn-0.24Fe-<0.1Si-0.02Cu-<0.01Cr (wt.%).

Uniaxial tensile tests were carried out at a cross-head speed of 0.9 mm/min (equivalent to a nominal strain rate of

This article was presented at Materials Science & Technology 2007, Automotive and Ground Vehicles symposium held September 16-20, 2007, in Detroit, MI.

Jidong Kang, School of Welding Engineering Technology, Northern College, 140 Government Road East, Kirkland Lake, ON, Canada P2N 3L8; **Jidong Kang, David S. Wilkinson,** and **J. David Embury**, Department of Materials Science and Engineering, McMaster University, 1280 Main street West, Hamilton, ON, Canada L8S 4L7; **Mike Bruhis, Mukesh Jain,** and **Pei Dong Wu**, Department of Mechanical Engineering, McMaster University, 1280 Main street West, Hamilton, ON, Canada L8S 4L7; and **Raja K. Mishra** and **Anil K. Sachdev**, Materials and Processes Lab, GM R&D Center, 30500 Mound Road, Warren, MI 48090-9055. Contact e-mail: kangj@northern.on.ca.

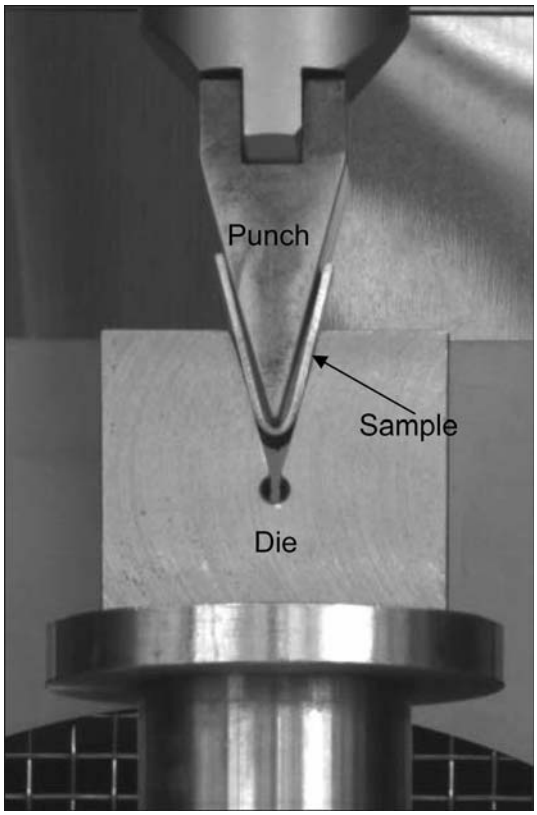

Fig. 1 Experimental setup for V-bending test

6×10^{-4} s^{-1}) on a 250 KN MTS tensile machine equipped with a TCE-N300 Shimadzu thermostatic chamber. The test temperature of the chamber can be maintained over the range of −70 °C to +280 °C using liquefied nitrogen injection and heater. The accuracy of the temperature distribution is 1.5 °C.

Previous results had shown that AA5754 sheet materials of similar chemical composition (Ref 8) do not exhibit PLC effect at 223 K at a strain rate of 6×10^{-4} s^{-1}. Tensile tests were conducted with simultaneous DIC data acquisition under three different conditions: (1) the tensile samples were pulled monotonically to fracture at 223 K, (2) the tensile samples were first pulled at 223 K to diffuse necking and unloaded, then reloaded to fracture at room temperature, (3) the tensile samples were first pulled at 223 K to localized necking and unloaded, then reloaded to fracture at room temperature. For comparison, tensile tests were also carried out at room temperature under identical test conditions.

The ARAMIS strain-mapping system based on digital image correlation (DIC) (Ref 8, 11, 12) was used to follow the deformation pattern during the tensile tests. DIC relies on the principle that the distribution of gray scale values over a rectangular area (facet) in the initial image corresponds to the distribution of gray scale values of the same area in the destination image through a 3-dimensional translation. A cumulative strain map can be obtained by comparing successive images from a deformed sample with the initial image, while an incremental strain map can be computed by comparing the image at the current load step with the image recorded just before the current load increment. The accuracy of strain measurement by this technique has a maximum absolute error of 0.0025 strain regardless of the measured strain range. Details

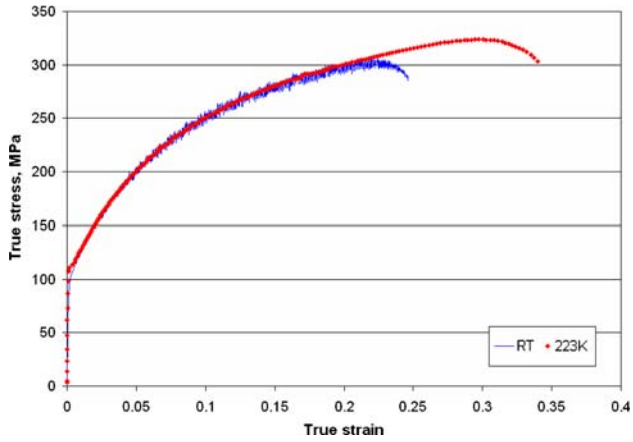

Fig. 2 Uniaxial tensile curves of continuous cast AA5754 at room temperature and 223 K at a strain rate of 6×10^{-4} s^{-1}. Note the absence of serrations in the data taken at 223 K

of the method are described in Ref 11 and 13. This system was also used to obtain the strain during in situ deformation using the V-bending fixture.

In the V-bending fixture (Fig. 1), a V-type punch is moved toward the corresponding die during the bending process. The advantage of this setup is to maintain a fixed view window for recording images for digital image correlation so that the camera can remain fixed during testing.

Considering the excellent bendability of AA5754 sheet material, to ensure rupture of the V-bending samples, a 200-mm (8″)-long and 100-mm (4″)-wide sample was prestrained to 10% by tensile loading along the long axis. V-bending samples (12-mm wide and 40-mm long) were machined from the prestrained samples with their length direction (40 mm) along the tensile axis. The ruptured tensile and bending samples were collected and mechanically polished to observe possible damage using light microscope.

2. Results and Discussion

Figure 2 shows the true stress-strain curves of samples deformed at room temperature and at 223 K to fracture. No serrations are observed on the tensile curve corresponding to the 223 K test, but are present at room temperature. From the strain-mapping results, it is also confirmed that no PLC bands were formed at this combination of temperature and strain rate (Fig. 3). However, inhomogeneous deformation was revealed at fairly small strains in the DIC maps. A noticeable finding is that several spots (red (black in B/W printing) dots with higher local strains in Fig. 3) form early during the deformation process. The formation of a diffuse shear band at a true strain of 0.30 and localized shear band at a true strain of 0.35 are found to be connected with the red spots (Fig. 3). The actual size of these red spots is in the order of 0.30×0.30 mm^2 as measured using the DIC map. These spots are thereafter refereed to as "hot spots".

The "hot spots" are local fluctuations in strain. Their size is larger than the grain size but limited by the resolution of DIC whether they are indeed grains in specific orientations is not clear and is under investigation. Our earlier results (Ref 8) from

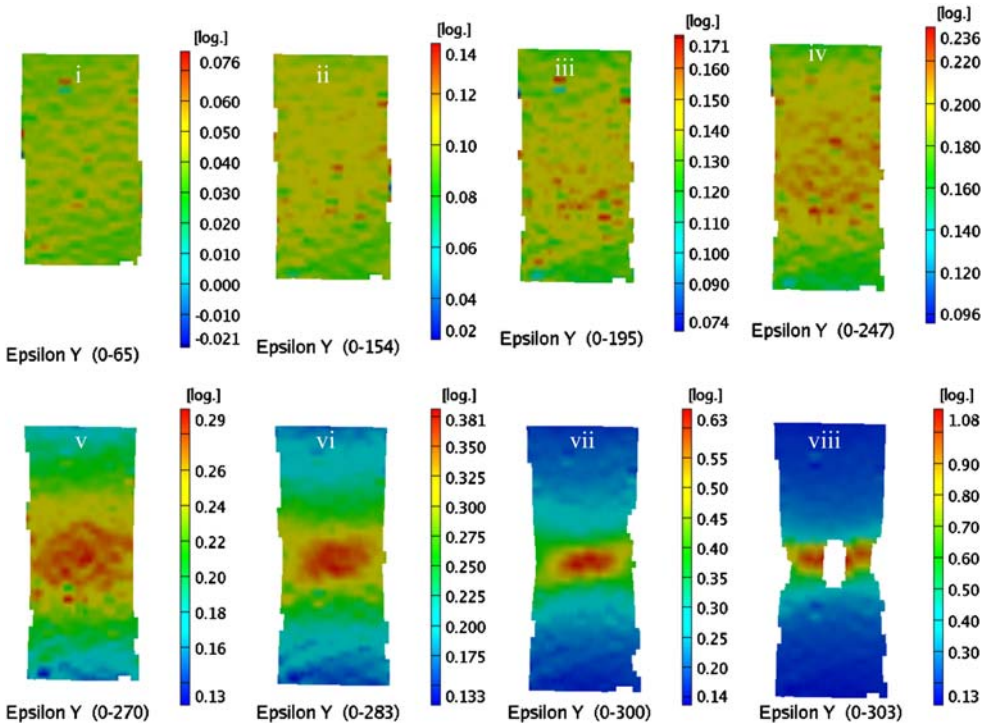

Fig. 3 DIC map showing axial strain distribution in a continuous cast AA5754 tensile sample tested at 223 K. Note the development of hot spots (in red color spots starting in panel ii) leading to the formation of localized necking band (panel v) and final fracture (panel viii) as deformation proceeds

field-emission scanning electron microscope (FE-SEM) showed that during tensile deformation, slip bands remain confined within individual grains, extending up to the grain boundary, and the strain distribution is inhomogeneous within the material. Similar findings have been reported for the initiation of adiabatic shear bands (Ref 14) as shown schematically in Fig. 4. The origin of shear bands has been suggested (Ref 14) to be due to one or more of the following as shown schematically in Fig. 4: (a) grain-size inhomogeneity, (b) geometrical softening, (c) Peirce-Asaro-Needleman textural localization (Ref 15, 16), and/or (d) dislocation pile-up (Ref 17) followed by their release. Inhomogeneities such as second-phase particle distribution and imperfection can also act as sites for shear band formation. Crystal plasticity simulations (Ref 18) have shown that shear bands can form in aluminum sheets with a uniform grain size and random distribution of orientations (one grain represented by one element of the same size) due to nonhomogeneous deformation. The data in Fig. 3 corroborate the view that shear band formation has its origin in the inhomogeneous deformation of the material, manifested in local "hot spots" in Fig. 3.

The "hot spot" phenomenon was observed in all the samples tested at 223 K. At room temperature, hot spots could not be distinguished from PLC bands. To delineate the relationship between PLC bands and shear bands, we tested some tensile samples to diffuse necking and some samples to localized necking at 223 K under conditions where no PLC bands form and then reloaded them at room temperature where PLC effect appears.

When diffuse neck forms at 223 K, many hot spots collectively organize themselves to form the wide band structure in an area of the sample (Fig. 5a). When reloaded at

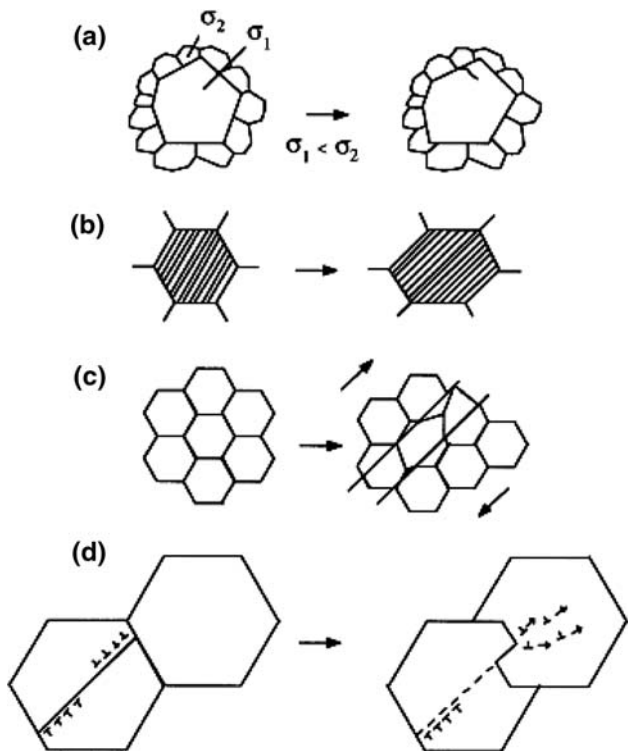

Fig. 4 Possible shear band initiation mechanisms in single-phase homogeneous materials. (a) grain-size inhomogeneity, (b) geometrical softening, (c) Peirce-Asaro-Needleman textural localization, and (d) dislocation pile-up release (After Ref 14). Schematic on the right side shows the shear band initiation as a result

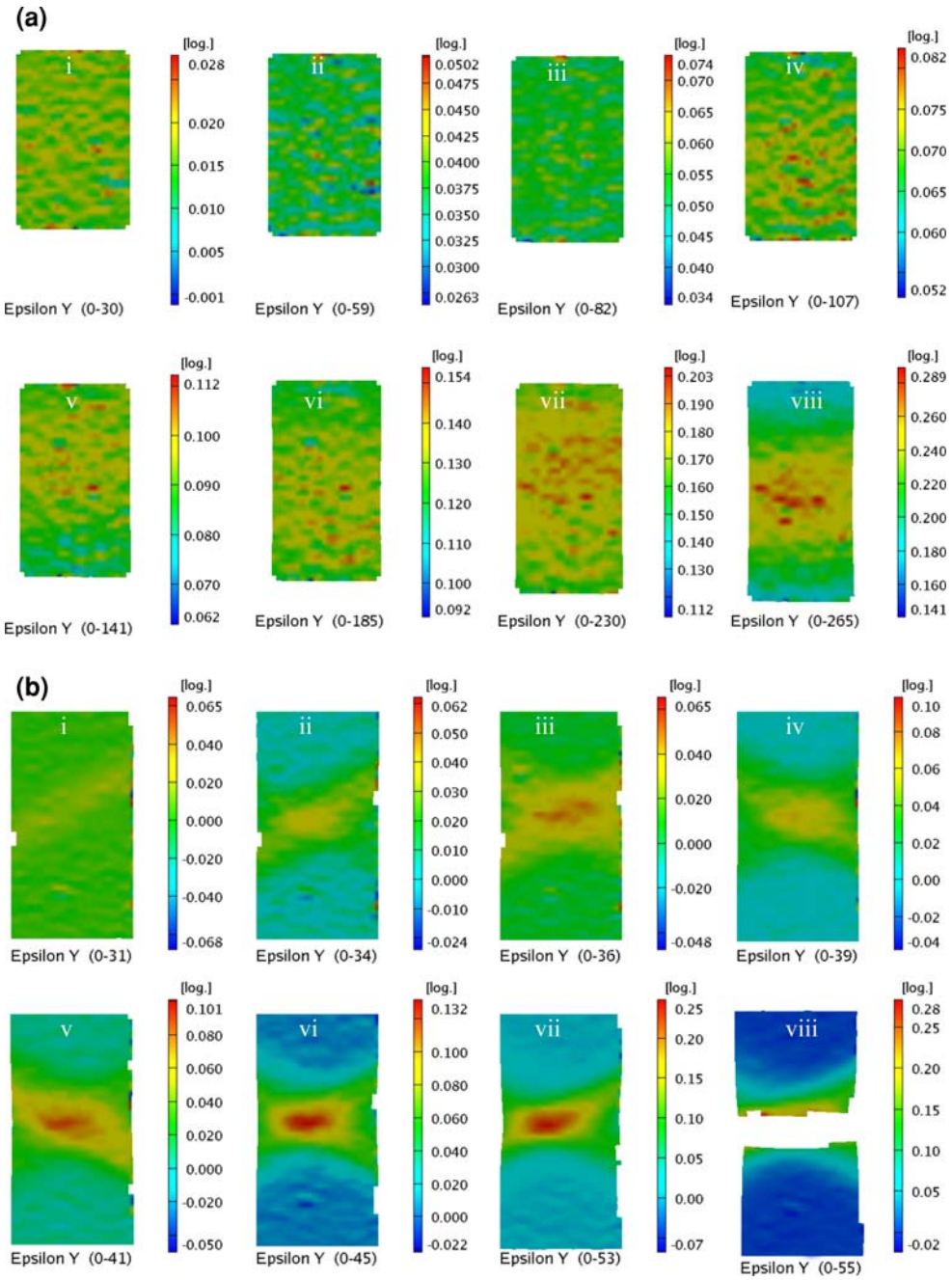

Fig. 5 (a) DIC map of axial strain distribution in a continuous cast AA5754 uniaxial tensile sample tested up to diffuse necking at 223 K. Note the development of hot spots (in red color) leading to diffuse neck band in panel viii and (b) strain distribution in the sample as it is reloaded to fracture at room temperature. Note that the PLC bands (band strain 0.02) detected the prior hot spots and localized the shear band on them, leading to final fracture

room temperature, it is seen that PLC bands first appear within the previous diffuse neck area. However, it is not clear whether these PLC bands are associated with "hot spots" (Fig. 5b).

We then tested the sample further to localized neck at 223 K and found a groove is formed on both sides of the tensile sample, i.e., the weak spot remains on the sample (Fig. 6a) after reloading. When this sample is reloaded at room temperature, it is not surprising to see that PLC bands first initiate at the grooved neck region where stresses would be higher, followed by shear band formation and final fracture (Fig. 6b) at the site of the localized neck.

From these tests, it can be concluded that PLC bands detect local strain concentrators and provide sites for shear bands. Similar conclusions were drawn by Yoshida and Toyooka (Ref 19) using electronic speckle pattern interferometry (ESPI). Yoshida and Toyooka (Ref 19) found a band structure that was referred to as a "decorrelation band" (DB), identical to PLC bands in our case. They concluded that the DB could be regarded as an indicator of local stress concentration that ultimately develops to failure.

The sequence of damage and shear band formation has been unambiguously established to be damage nucleation (voiding)

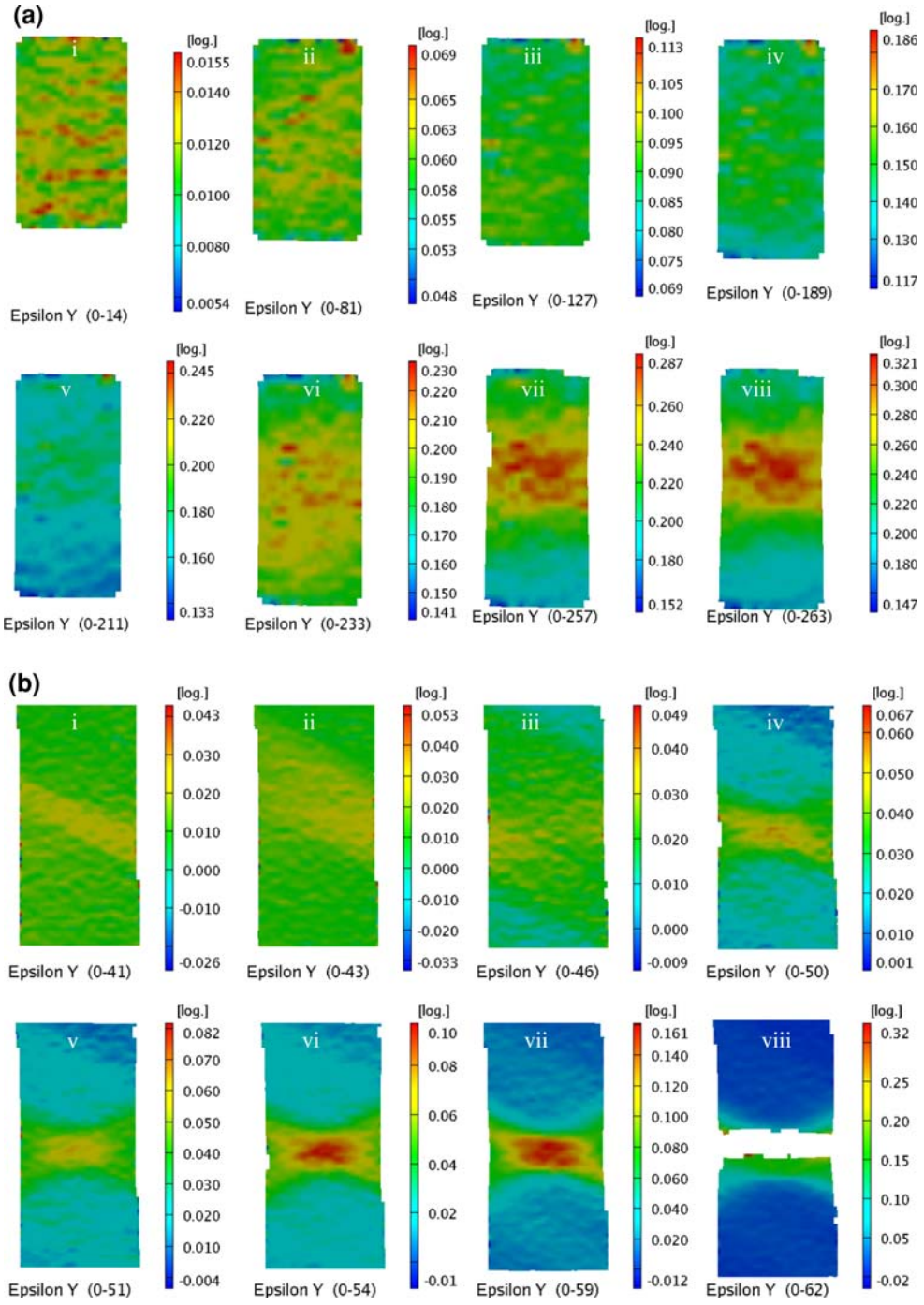

Fig. 6 DIC map of axial strain distribution in CC AA5754 uniaxial tensile sample tested up to localized necking at 223 K. The hot spots (in red color in panel i) lead to diffuse neck (panel vi) and localized bands (panel viii) and (b) DIC map of the same sample unloaded and then reloaded to fracture at room temperature. PLC bands detect the site of localized neck and shear bands initiated there leading to the final fracture

followed by shear band localization before fracture. Attempts to find evidence for the same mechanisms have been unsuccessful. Gurson and modified Gurson models (Ref 20, 21) accounting for mechanisms similar to those in steel have been unable to reproduce experimental data for aluminum alloys. In 5xxx series aluminum alloys, there is experimental evidence that shear bands form prior to damage (Ref 7-9, 22) or void formation. We use bending tests to clarify the sequence of damage and shear band formation in aluminum. Unlike tensile deformation, no necks form before fracture during bending (plain strain deformation). From V-bending tests of the samples, it can be seen in Fig. 7 that damage occurs at an equivalent true strain of 0.65 (after accounting for the 10% tensile prestrain), much larger than the necking point (true strain of 0.35) in tensile sample. In other words, shear banding in tensile samples occurs prior to damage (void formation) and damage occurs inside the shear bands when local strain rises to a value of ~0.65. Figure 8 shows the damage in the midsection

of a partially fractured bent sample, polished to reveal voids and cracks. It is seen in Fig. 8 that the fracture path follows along the stringers and jumps between stringers. The stringer locations can be considered to be where voids form locally even though they are not resolved at this image magnification (Ref 23).

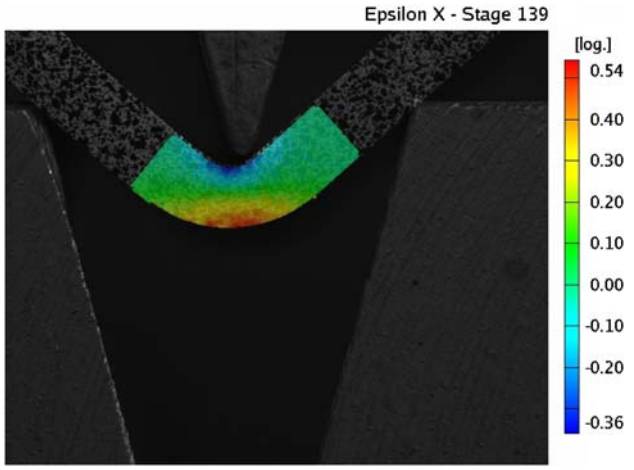

Fig. 7 Strain distribution in a continuous cast AA5754 sample subjected to V-bending. Note the high strain value compared to that in the localized bands in the tensile sample above without any fracture initiation

All the above observations, taken together with data in the literature, lead us to conclude that the following sequence of events must be incorporated into modeling deformation and fracture of aluminum alloys: (a) strain localization occurs at small deformation due to nonhomogeneous nature of plastic flow in polycrystalline and multiphase aluminum sheets, (b) PLC bands (under appropriate strain rate and temperature conditions) associate themselves with the local strain centers, (c) shear bands arise from geometric inhomogeneities and PLC bands connect with shear bands and localize them, (d) stringers and particles in the shear band provide damage sites, and (e) damage sites in the shear band get connected to cause final failure.

3. Conclusions

Experimental results from tensile tests at 223 K and room temperature show that PLC bands detect and provide the sites for shear banding. In situ V-bending tests coupled with deformation mapping based on digital image correlation show that damage occurs at much higher strain than the necking strain in tensile samples. The data confirm that the formation of shear bands occurs prior to damage, i.e., damage is a consequence of shear band formation. This mechanism can guide modeling of shear localization in AA5754 sheet materials.

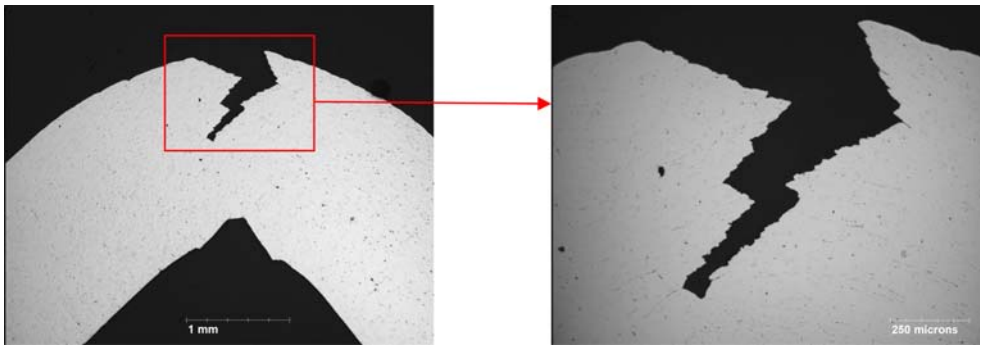

Fig. 8 Damage in a continuous cast AA5754 sample deformed to failure in the V-bending fixture. There are no voids away from the fracture surface and the crack moves from stringer to stringer at this resolution

Acknowledgments

Many valuable discussions with research personnel at General Motors R&D Center are gratefully acknowledged. The financial support of General Motors of Canada Ltd and the Natural Sciences and Engineering Research Council of Canada is gratefully acknowledged.

References

1. J.E. Bird, K.E. Newman, K. Narasimhan, and J.M. Carlson, Heterogeneous Initiation and Growth of Sample-scale Shear Bands During Necking of Al-Mg Sheet, *Acta Metall.*, 1987, **35**, p 2971–2982
2. G.Y. Chin, W.F. Hosford, and W.A. Backofen, Ductile fracture of aluminum, *Trans. Met. Soc. AIME*, 1964, **230**, p 437–448
3. N. Chung, J.D. Embury, J.D. Evenson, R.G. Hoagland, and C.M. Sargent, Unstable Shear Failure in a 7075 Aluminum Alloy, *Acta Metall.*, 1977, **25**, p 377–381
4. P.W. Beaver, Localized Thinning, Fracture and Formability of Aluminum Sheet Alloys in Biaxial Tension, *J. Mech. Work. Tech.*, 1982-1983, **7**, p 215–231
5. A. Korbel, J.D. Embury, M. Hatherly, P.L. Martin, and H.W. Erbsloh, Microstructural Aspects of Strain Localization in Al-Mg Alloys, *Acta Metall.*, 1986, **34**, p 1999–2009
6. Viewpoint Set No. 6: Shear Bands, *Scripta Metall.*, 1984, **18**, p 421
7. J. Kang, D.S. Wilkinson, J.D. Embury, and K. Hussain, Investigation on Mechanism of Ductile Fracture of AA5754 Sheet, *Mater. Sci. Forum*, 2006, **519–521**, p 985–990
8. J. Kang, D.S. Wilkinson, D.V. Malakhov, H. Halim, M. Jain, J.D. Embury, and R. Mishra, Effect of Processing Route on Spatial Distribution of Constituent Particles and Their Role in Fracture Process in Aluminum AA5754 Sheet Materials, *Mater. Sci. Eng. A*, 2007, **456**, p 85–92
9. J. Kang, D.S. Wilkinson, M. Jain, J.D. Embury, A.J. Beaudoin, S. Kim, R. Mishra, and A.K. Sachdev, On the Sequence of Inhomogeneous Deformation Processes Occurring During Tensile Deformation of Strip Cast AA5754, *Acta Mater.*, 2006, **54**, p 209–218
10. D. Lloyd, D. Evans, C. Pelow, P. Nolan, and M. Jain, Bending in Aluminum Alloys AA6111 and AA5754 Using the Cantilever Bend Test, *Mater. Sci. Technol.*, 2002, **18**(6), p 621–628
11. H.A. Bruck, S.R. McNeill, M.A. Sutton, and W.H. Peters III, Digital Image Correlation Using Newton-Raphson Method of Partial Differential Correlation, *Exp. Mech.*, 1982, **39**(3), p 261–267
12. J. Kang, D.S. Wilkinson, J.D. Embury, and M. Jain, Local Strain Measurement in a Strip Cast Automotive Aluminum Alloy Sheet, *SAE Trans.: J. Mater. Manuf.*, 2005, **114**, p 156–165
13. Aramis v4.7 manual, GOM mbH, Braunschweig, Germany, 2001
14. V.F. Nesterenko, M.A. Meyers, and T.W. Wright, Self-Organization in the Initiation of Adiabatic Shear Bans, *Acta Mater.*, 1998, **46**(1), p 327–340
15. D. Peirce, R.J. Asaro, and A. Needleman, Material Rate Dependent and Localized Deformation in Crystalline Solids, *Acta Metall.*, 1983, **31**(12), p 1951–1976
16. L. Anand and S.R. Kalidindi, The Process of Shear Band Formation in Plane Strain Compression of fcc Metals: Effects of Crystallographic Texture, *Mech. Mater.*, 1994, **17**, p 223–243
17. R.W. Armstrong and F.J. Zerilli, Dislocation Mechanics Aspects of Plastic Instability and Shear Banding, *Mech. Mater.*, 1994, **17**, p 319–327
18. P.D. Wu, S.R. MacEwen, D.J. Lloyd, and K.W. Neale, A Mesoscopic Approach for Predicting Sheet Metal Formability, *Modell. Simul. Mater. Sci. Eng.*, 2004, **12**, p 511–527
19. S. Yoshida and S. Toyooka, Field Theoretical Interpretation on Dynamics of Plastic Deformation-Portevin-Le Chatellier Effect and Propagation of Shear Band, *J. Phys.: Condens. Matter*, 2001, **13**, p 6741–6757
20. F.A. McClintock, A Criterion for Ductile Fracture by Growth of Holes, *Trans. ASME J. Appl. Mech.*, 1968, **35**, p 363–371
21. A.L. Gurson, Continuum Theory of Ductile Rupture by Void Nucleation and Growth. I. Yield Criteria and Flow Rules for Porous Ductile Media, *J. Eng. Mater. Technol.*, 1977, **99**, p 2–15
22. J. Sarkar, T.R.G. Kutty, K.T. Conlon, D.S. Wilkinson, J.D. Embury, and D.J. Lloyd, Tensile and Bending Properties of AA5754 Aluminum Alloys, *Mater. Sci. Eng.*, 2001, **A316**, p 52–59
23. R. Raghavan, P. Biswas, and R. Mishra, Influence of Microstructure and Material Variables on Hemmability of Aluminum Alloys, *Acta Mater.*, submitted for publication